Electronic Supplementary Material (ESI) for Dalton Transactions.
This journal is © The Royal Society of Chemistry 2022

Supporting Information

Three Isostructural Hexanuclear Lanthanide-Organic Frameworks for Sensitive Luminescence Temperature Sensing Over a Wide Range

Tifeng Xia,*[ab] Wenqian Cao,[b] Lingling Guan,[b] Jun Zhang,*[a] Fudong Jiang,[a] Libing Yu,[a] and Yating Wan,*[c]

[a] *Institute of Materials, China Academy of Engineering Physics, Mianyang 621907, China. E-mail: xiatifeng@caep.cn (T. Xia), j-zhang@caep.cn (J. Zhang)*

[b] *State Key Laboratory of Silicon Materials, Cyrus Tang Center for Sensor Materials and Applications, School of Materials Science and Engineering, Zhejiang University, Hangzhou 310027, China.*

[c] *Shanghai Institute of Laser Plasma, China Academy of Engineering Physics, Shanghai 201800, China. E-mail: ytwan@zju.edu.cn*

Table S1 The molar ratio of the starting Eu/Tb salt and that in isomorphic Eu^{3+}/Tb^{3+} co-doped MOFs calculated by ICP analyses.

Samples	Tested Eu by ICP analysis (ppm)	Tested Tb by ICP analysis (ppm)	The Eu/Tb ratios calculated by ICP analysis
$Eu_{0.001}Tb_{0.999}$-0N	0.3233	124.1	0.0026:0.9974
$Eu_{0.001}Tb_{0.999}$-1N	0.0673	38.94	0.0017:0.9983
$Eu_{0.001}Tb_{0.999}$-2N	0.1002	32.80	0.0030:0.9970

Table S2 Fitting parameters of isomorphic Eu^{3+}/Tb^{3+} mixed MOFs with double exponential Mott-Seitz model.

Ln-MOFs	Δ_0	α_1	ΔE_1	α_2	ΔE_2	R^2
$Eu_{0.001}Tb_{0.999}$-0N[a]	1.14611	4.93616	121.858	196.053	630.975	0.9986
$Eu_{0.001}Tb_{0.999}$-0N[b]	14.9587	4.9435	121.988	196.558	631.520	0.9986
$Eu_{0.001}Tb_{0.999}$-1N[a]	1.18613	45.3146	101.299	3032.19	573.568	0.9999
$Eu_{0.001}Tb_{0.999}$-1N[b]	299.108	45.1351	101.457	3021.64	573.990	0.9999
$Eu_{0.001}Tb_{0.999}$-2N[a]	3.37050	9.48916	48.1217	2677.79	679.935	0.9996
$Eu_{0.001}Tb_{0.999}$-2N[b]	136.870	9.1291	48.7506	2589.08	680.871	0.9996

[a] Normalized to 50 K; [b] Normalized to 300 K.

Table S3 A summary of some reported ratiometric MOF-based thermometers.

Luminescent MOF	Range (K)	S_m (%·K^{-1})	T_m (K)
$Eu_{0.001}Tb_{0.999}$(BPDC-0N)	**50-300**	**1.10**	**188**
$Eu_{0.001}Tb_{0.999}$(BPDC-1N)	**50-300**	**4.11**	**50**
$Eu_{0.001}Tb_{0.999}$(BPDC-2N)	**50-300**	**1.94**	**50**
9.1wt%EuW_{10}@Tb-TATB[1]	200-320	2.68	300
19.5wt%EuW_{10}@Tb-TATB[1]	200-320	2.37	300
$Tb_{0.99}Eu_{0.01}(bdc)_{1.5}$ (in water)[2]	290-320	0.31	318
$Tb_{0.99}Eu_{0.01}(bdc)_{1.5}$ (solid)[2]	290-320	0.14	318
Dycpia[3]	298-473	0.42	473
ZJU-88⊃perylene[4]	293-353	1.28	293
$[Tb_{0.970}Eu_{0.030}(CH_3COO)(1,3\text{-bdc})(H_2O)]$[5]	150-350	0.19	338
$[Tb_{0.950}Eu_{0.050}(CH_3COO)(1,3\text{-bdc})(H_2O)]$[5]	150-350	0.20	333
$[Tb_{0.925}Eu_{0.075}(CH_3COO)(1,3\text{-bdc})(H_2O)]$[5]	150-350	0.24	314
$[Tb_{0.900}Eu_{0.100}(CH_3COO)(1,3\text{-bdc})(H_2O)]$[5]	150-350	0.31	284
$[Tb_{0.875}Eu_{0.125}(CH_3COO)(1,3\text{-bdc})(H_2O)]$[5]	150-350	0.40	251
$[Tb_{0.850}Eu_{0.150}(CH_3COO)(1,3\text{-bdc})(H_2O)]$[5]	150-350	0.44	236
Cdots&RB@ZIF-82-MMM-1[6]	293-353	0.74	293
$Eu_{0.0025}Tb_{0.9975}$-BABDC-PBMA[7]	90-240	3.61	240

Table S4 Crystallographic Data Collection and Refinement Results for **Eu(BPDC-2N)**.

Sample	**Eu(BPDC-2N)**
Chemical formula	$C_{72}H_{45}Eu_6F_8N_{12}O_{27.50}$
Formula weight	2581.96
Temperature (K)	173
Wavelength (Å)	0.71073
Crystal system	Cubic
Space group	Fm-3m
a (Å)	27.498(6)
b (Å)	27.498(6)
c (Å)	27.498(6)
V (Å^3)	20792(15)
Z	4
Density (calculated g·cm^{-3})	0.825
Absorbance coefficient (mm^{-1})	1.824
F(000)	4924
Crystal size (mm^3)	0.12 × 0.11 × 0.10
R(int)	0.0464
Goodness of fit on F_2	1.029
R_1,wR_2[I>2σ(I)][a]	0.0259, 0.0734
R_1,wR_2(all data)[a]	0.0276, 0.0744
Largest difference peak and hole (e Å^{-3})	0.555, -0.660

[a] $R1 = \sum\left(|F_o| - |F_c|\right)/\sum|F_o|; wR2 = \left[\frac{\sum w\left(|F_o| - |F_C|^2\right)}{\sum wF_o^2}\right]^{1/2}$

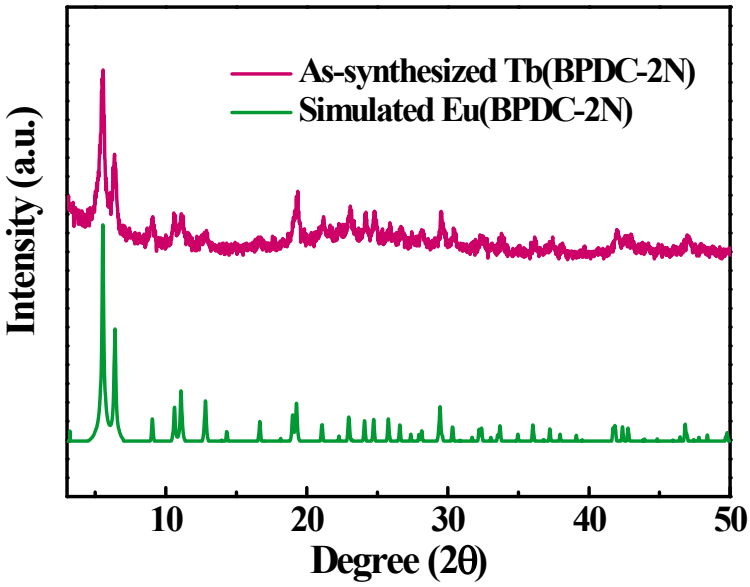

Figure S1. The PXRD patterns of simulated Eu(BPDC-2N) and as-synthesized Tb(BPDC-2N).

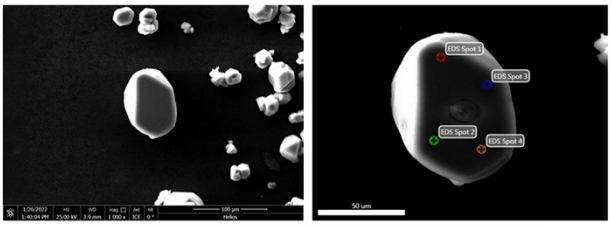

Elements	Spot 1	Spot 2	Spot 3	Spot 4
C (mol%)	85.79	67.61	68.64	70.04
N (mol%)	0.40	13.44	12.87	11.95
O (mol%)	4.43	12.95	12.92	12.20
Eu (mol%)	9.38	6.00	5.56	5.81

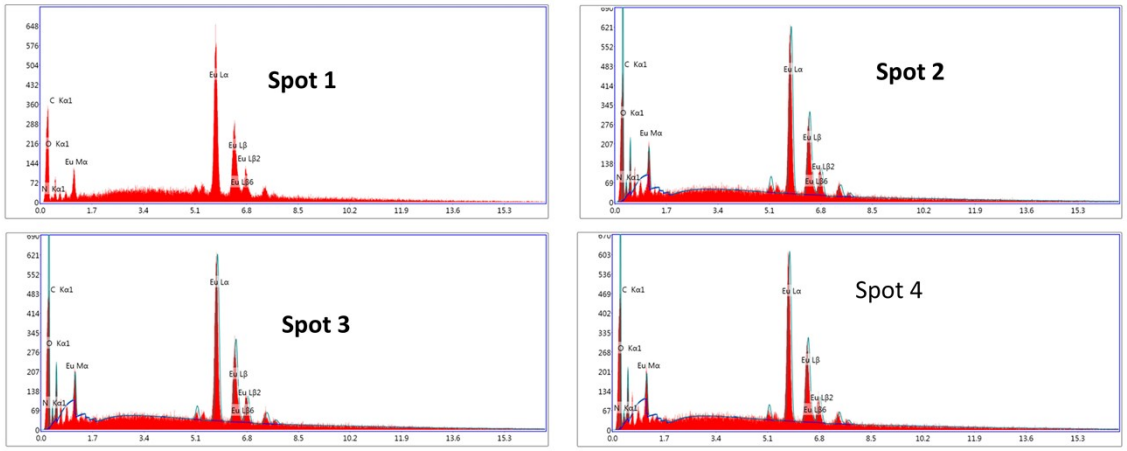

Figure S2. SEM and SEM-EDX of Eu(BPDC-2N).

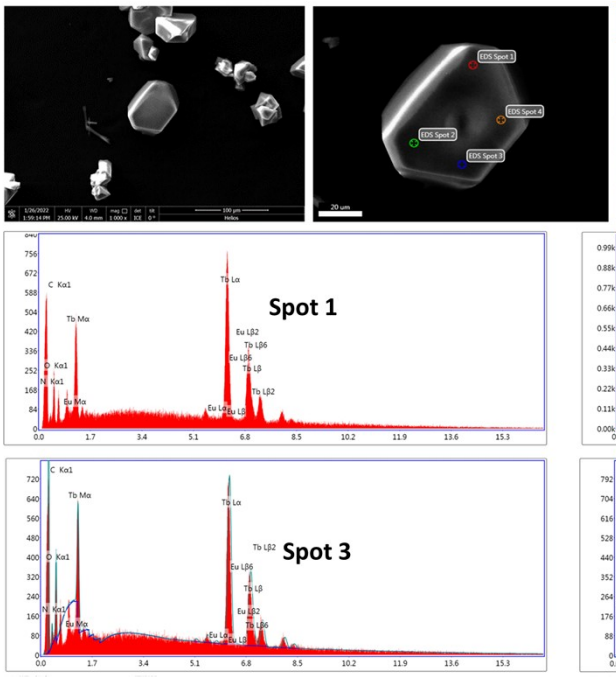

Elements	Spot 1	Spot 2	Spot 3	Spot 4
C (mol%)	74.61	63.56	63.70	68.77
N (mol%)	7.10	14.77	14.72	10.81
O (mol%)	12.29	18.05	17.28	15.25
Eu (mol%)	0.09	0.05	0.07	0.05
Tb (mol%)	5.92	3.56	4.23	5.12

Figure S3. SEM and SEM-EDX of $Eu_{0.001}Tb_{0.999}$(BPDC-2N).

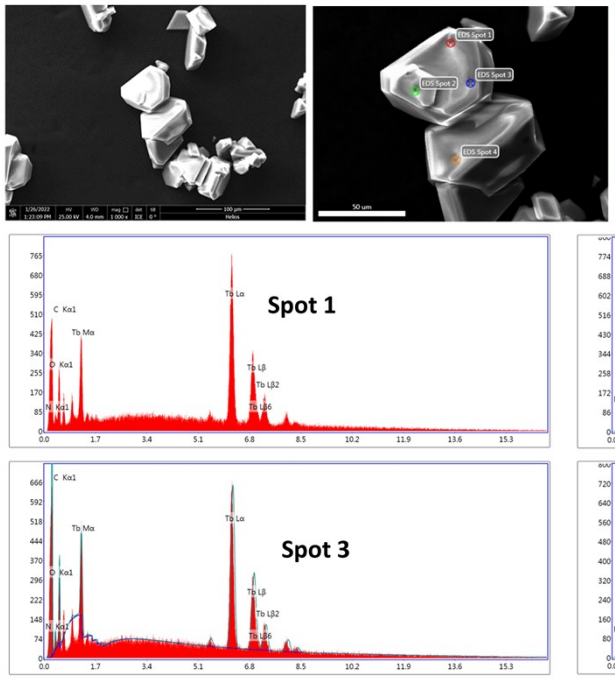

Elements	Spot 1	Spot 2	Spot 3	Spot 4
C (mol%)	65.07	60.85	64.52	64.45
N (mol%)	12.71	15.91	13.87	14.50
O (mol%)	16.18	18.92	17.38	16.11
Tb (mol%)	6.04	4.33	4.23	4.95

Figure S4. SEM and SEM-EDX of Tb(BPDC-2N).

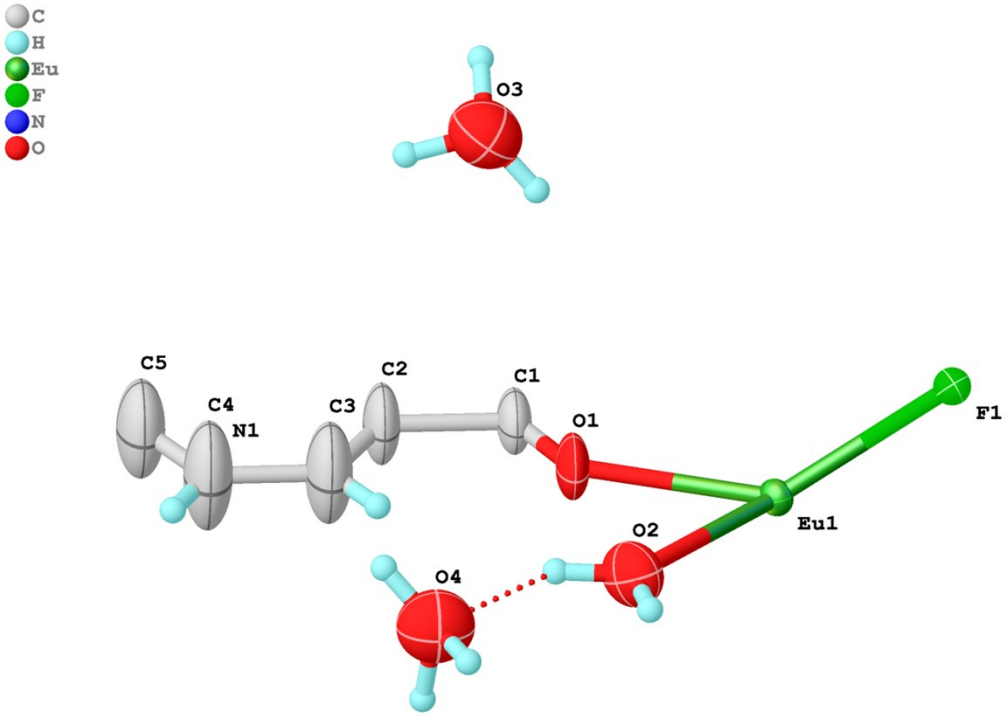

Figure S5. Ortep representation of the asymmetric unit in Eu(BPDC-2N) (50% probability factor for the thermal ellipsoids).

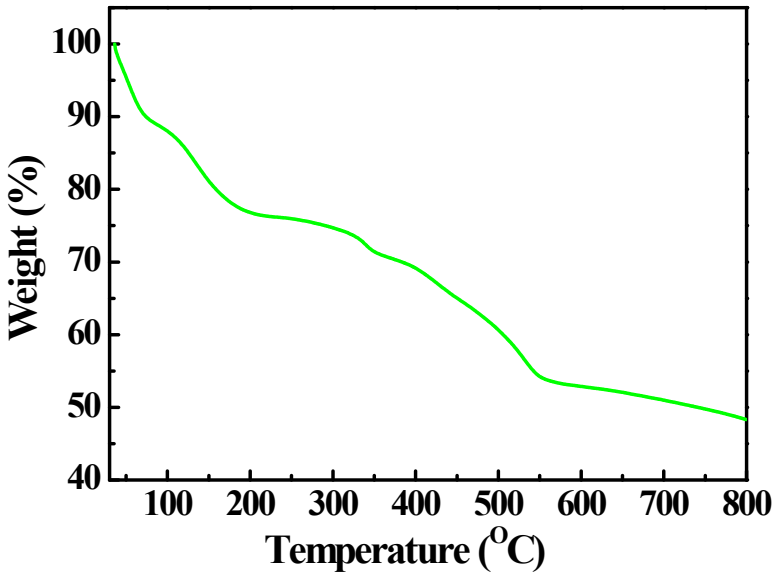

Figure S6. TGA curves of Eu(BPDC-2N).

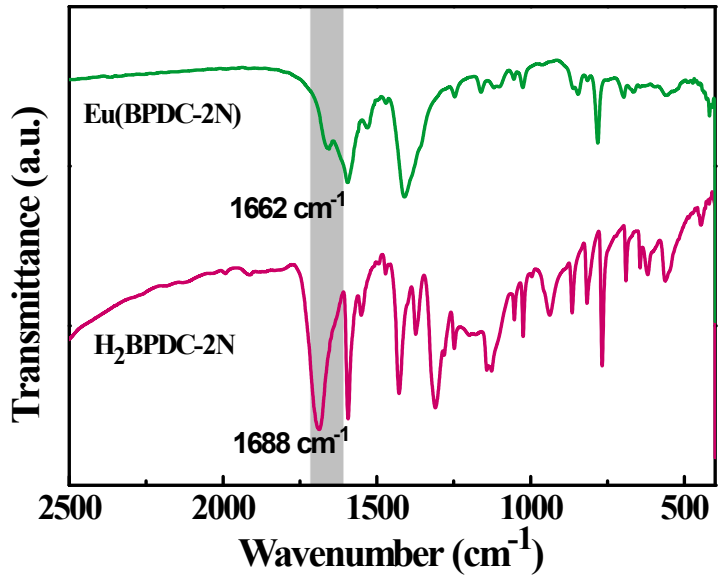

Figure S7. FT-IR spectra of organic ligand H_2BPDC-2N and Eu(BPDC-2N).

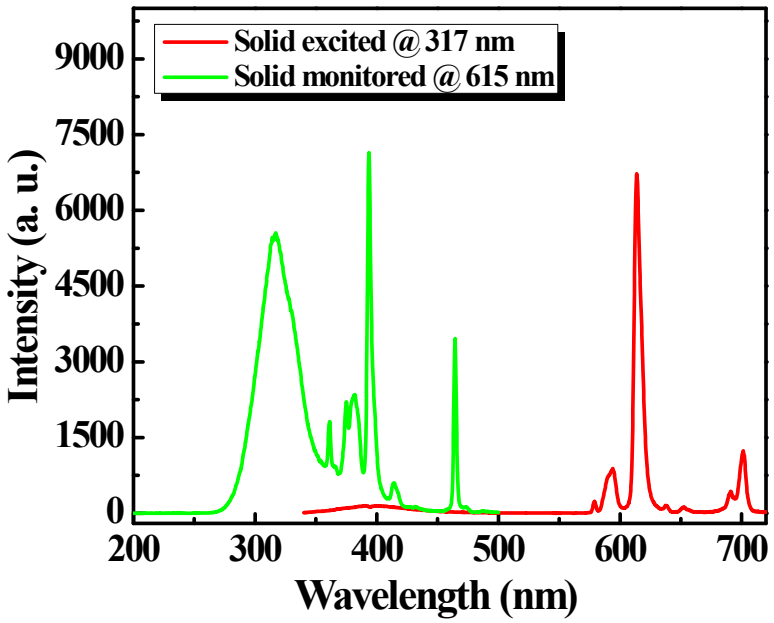

Figure S8. Excitation and emission spectra of Eu(BPDC-0N) at room temperature.

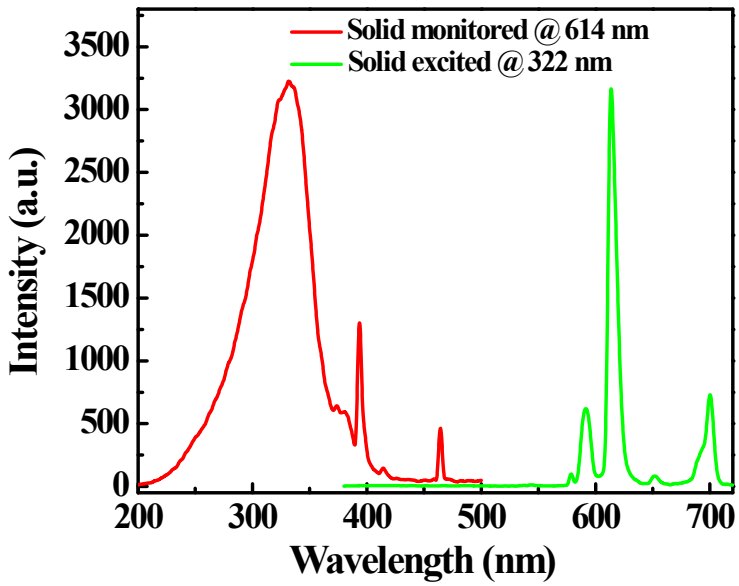

Figure S9. Excitation and emission spectra of Eu(BPDC-1N) at room temperature.

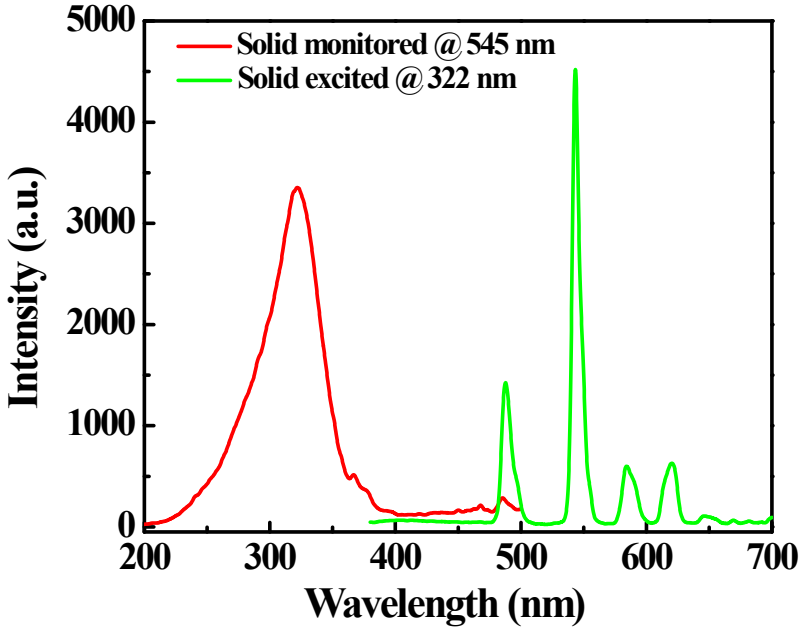

Figure S10. Excitation and emission spectra of Tb(BPDC-1N) at room temperature.

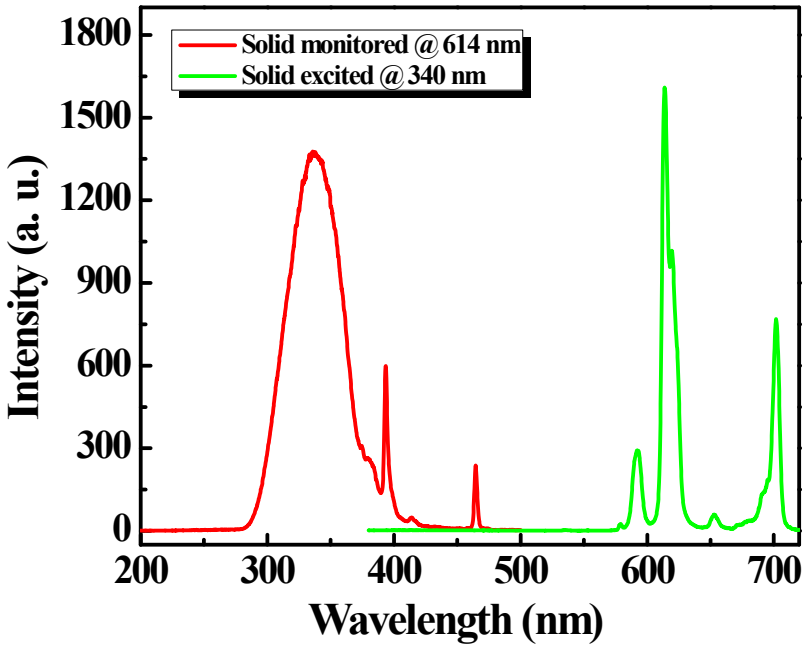

Figure S11. Excitation and emission spectra of Eu(BPDC-2N) at room temperature.

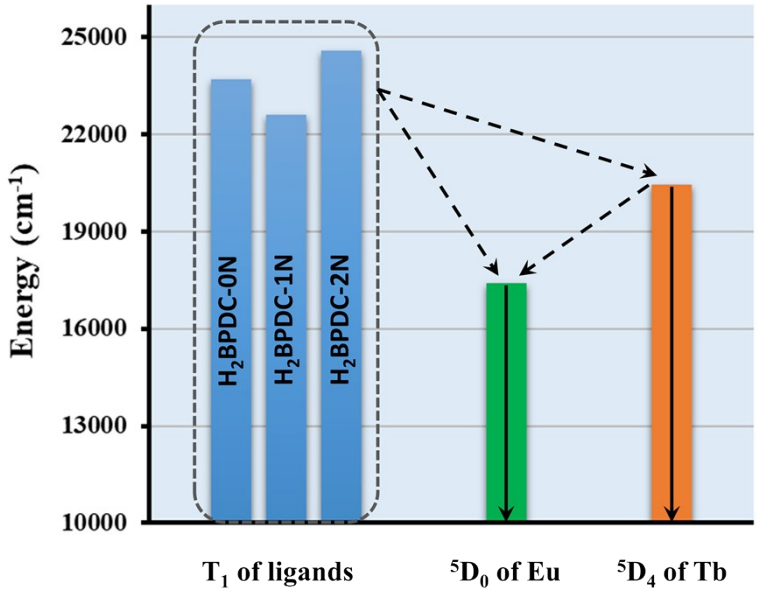

Figure S12. The calculated triplet levels of H_2BPDC-*x*N (*x* = 0, 1, 2) and energy levels of Eu ($^5D_0$) and Tb ($^5D_4$).

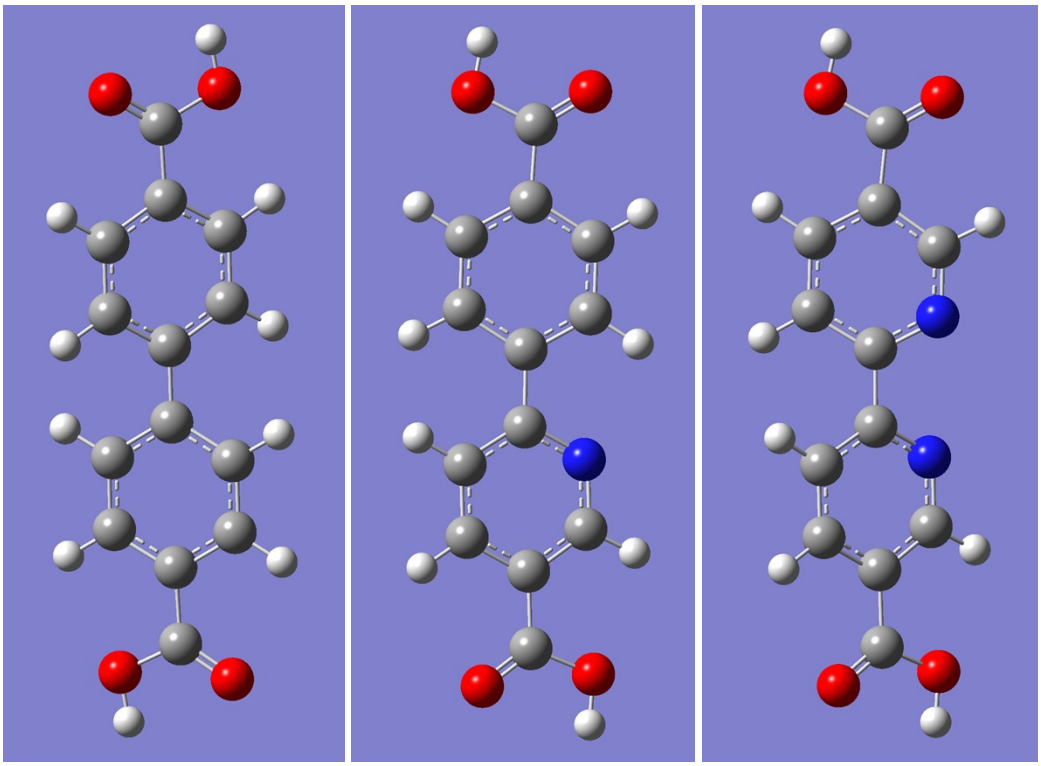

Figure S13. The optimized geometry of free ligands H_2BPDC-*x*N (*x* = 0, 1, 2) at the B3LYP/6-31G* level.

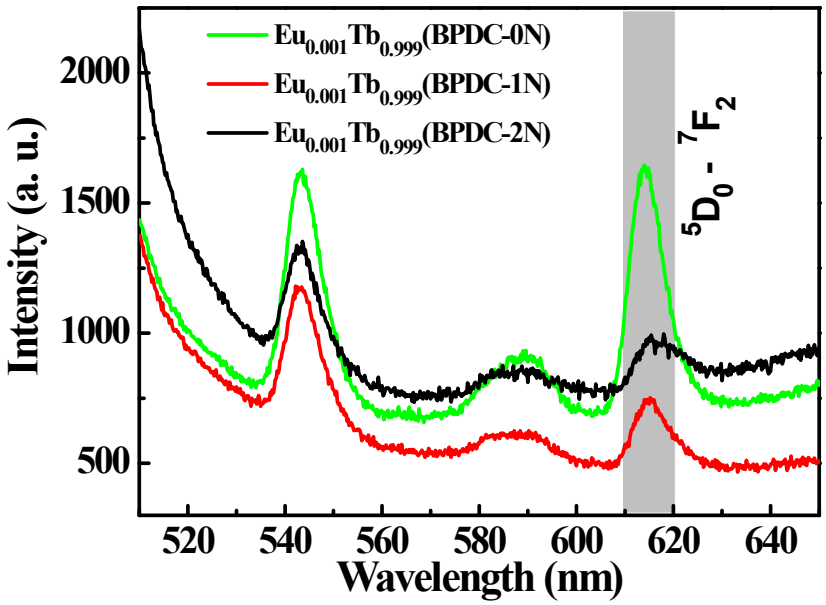

Figure S14. Emission spectra of $Eu_{0.001}Tb_{0.999}$(BPDC-*x*N) (*x* = 0, 1, 2) excited at 488 nm.

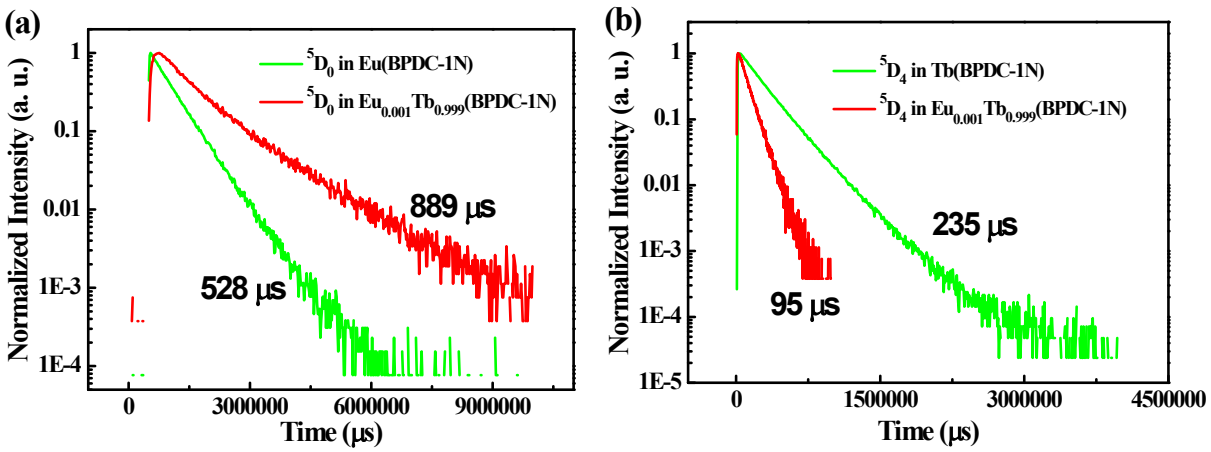

Figure S15. Fluorescence decay curves of $^5D_0$ (a) and $^5D_4$ (b) in Eu(BPDC-1N), Tb(BPDC-1N), and $Eu_{0.001}Tb_{0.999}$(BPDC-1N).

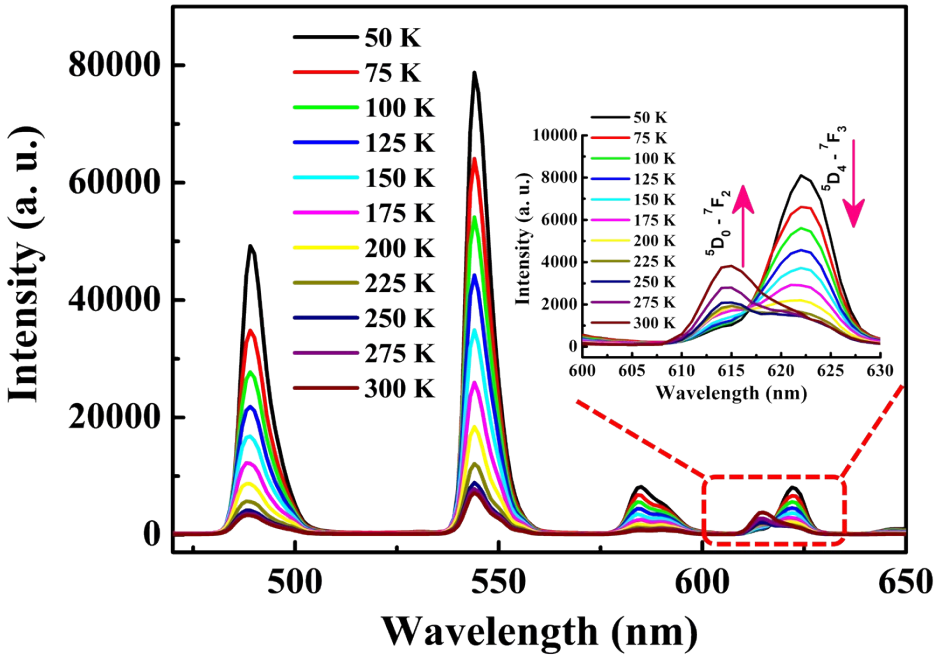

Figure S16. Temperature-dependent emission spectra of $Eu_{0.001}Tb_{0.999}$(BPDC-2N) in the temperature range from 50 K to 300 K.

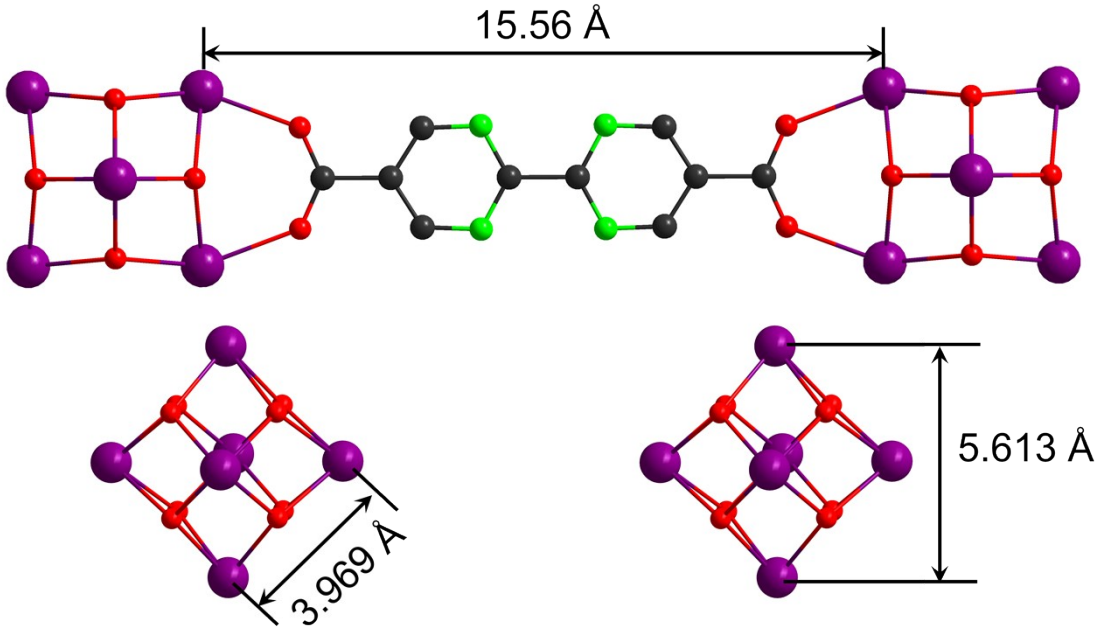

Figure S17. The shortest distance of two lanthanide ions in the adjacent SBUs and two possible distances between Tb^{3+} and Eu^{3+} in the same SBU.

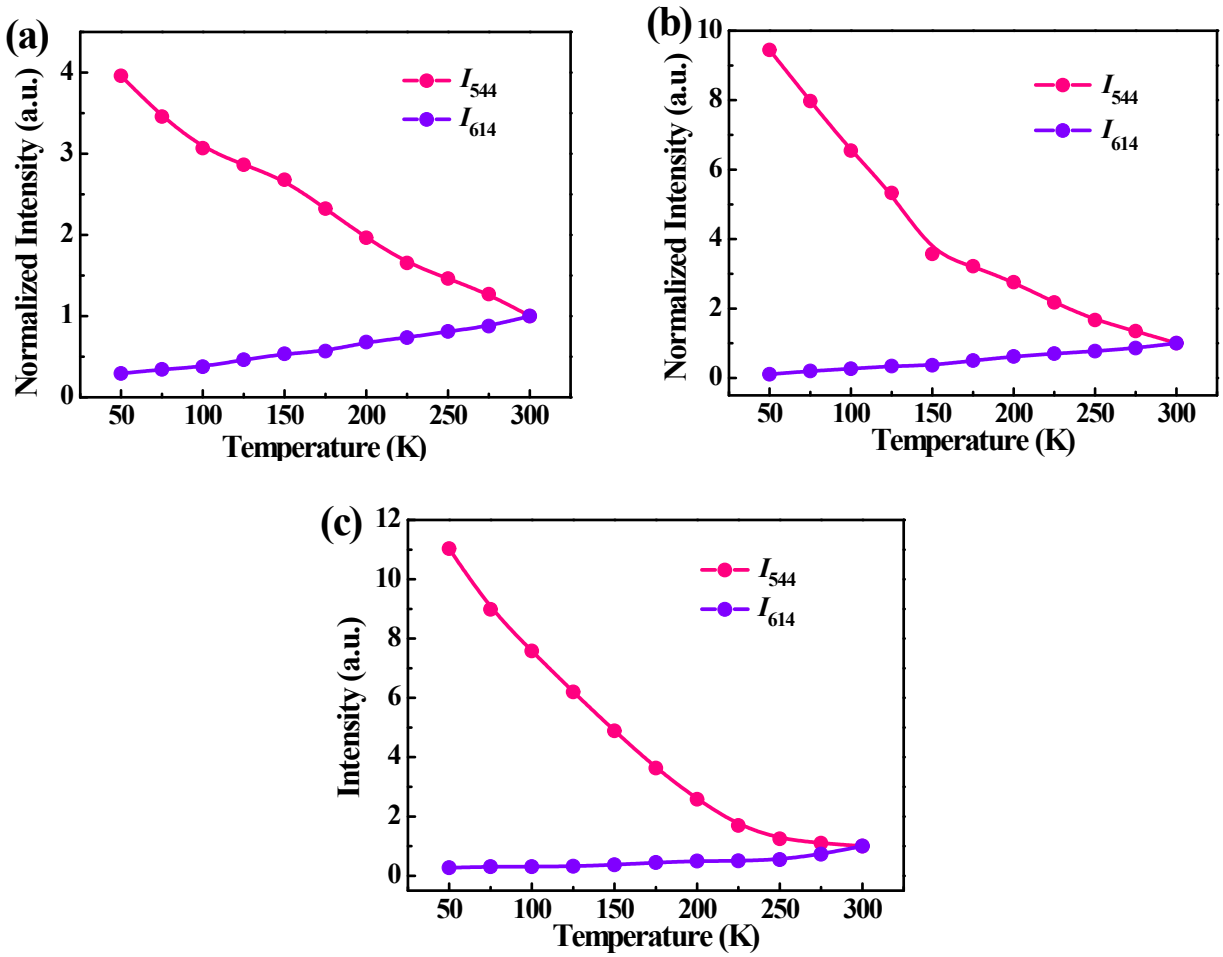

Figure S18. Normalized luminescence intensity of $^5D_4$ - $^7F_5$ transition and $^5D_0$ - $^7F_2$ transition for (a) $Eu_{0.001}Tb_{0.999}$(BPDC-0N), (b) $Eu_{0.001}Tb_{0.999}$(BPDC-1N) and (c) $Eu_{0.001}Tb_{0.999}$(BPDC-2N), respectively.

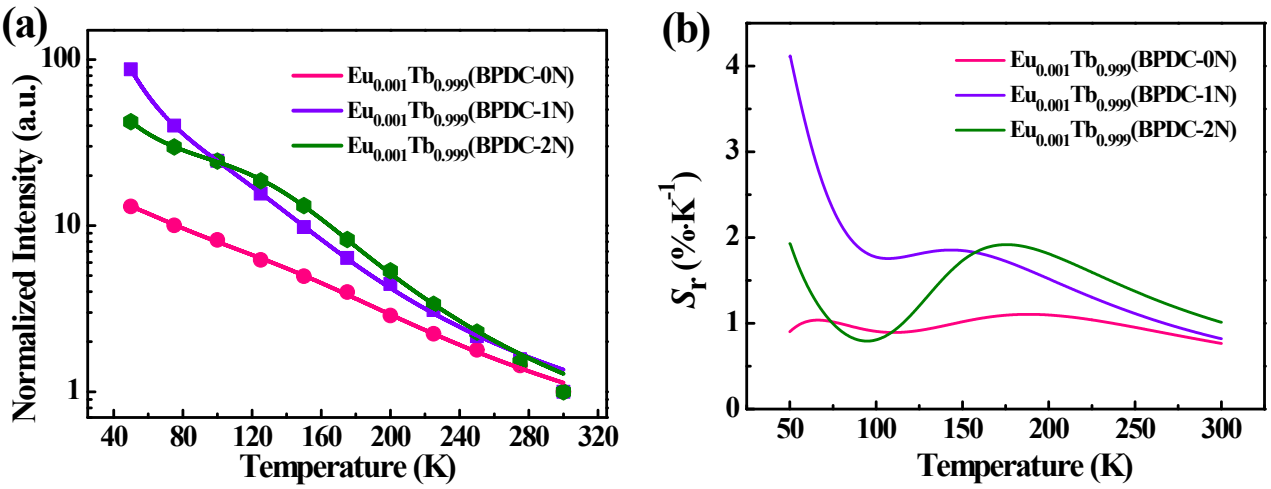

Figure S19. The fitting curves (a) and temperature-dependent relative sensitivity (b) of $Eu_{0.001}Tb_{0.999}$(BPDC-*x*N) (*x* = 0, 1, 2) when luminescence intensities were normalized to the intensity at 300 K.

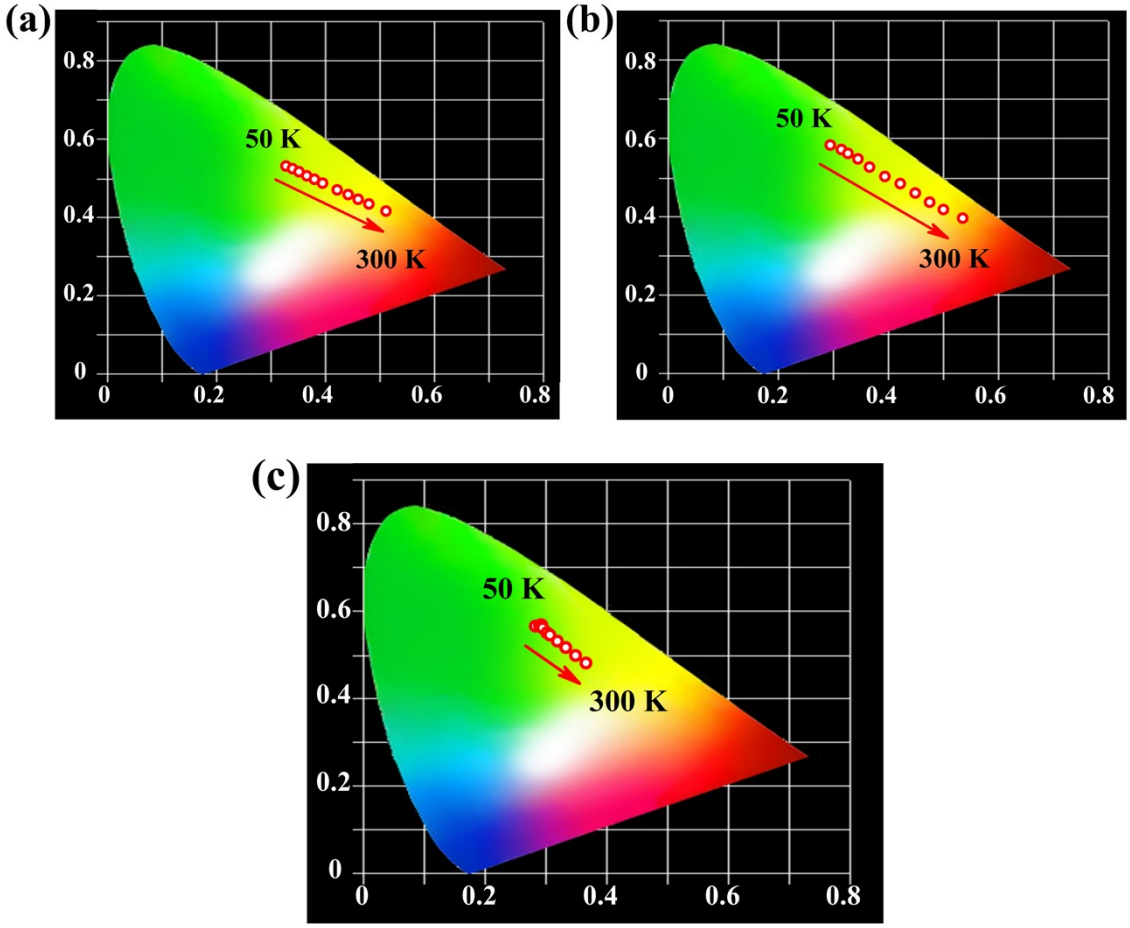

Figure S20. CIE chromaticity diagram presenting the temperature-dependent color of (a) $Eu_{0.001}Tb_{0.999}$(BPDC-0N), (b) $Eu_{0.001}Tb_{0.999}$(BPDC-1N) and (c) $Eu_{0.001}Tb_{0.999}$(BPDC-2N) in the temperature range from 50 K to 300 K.

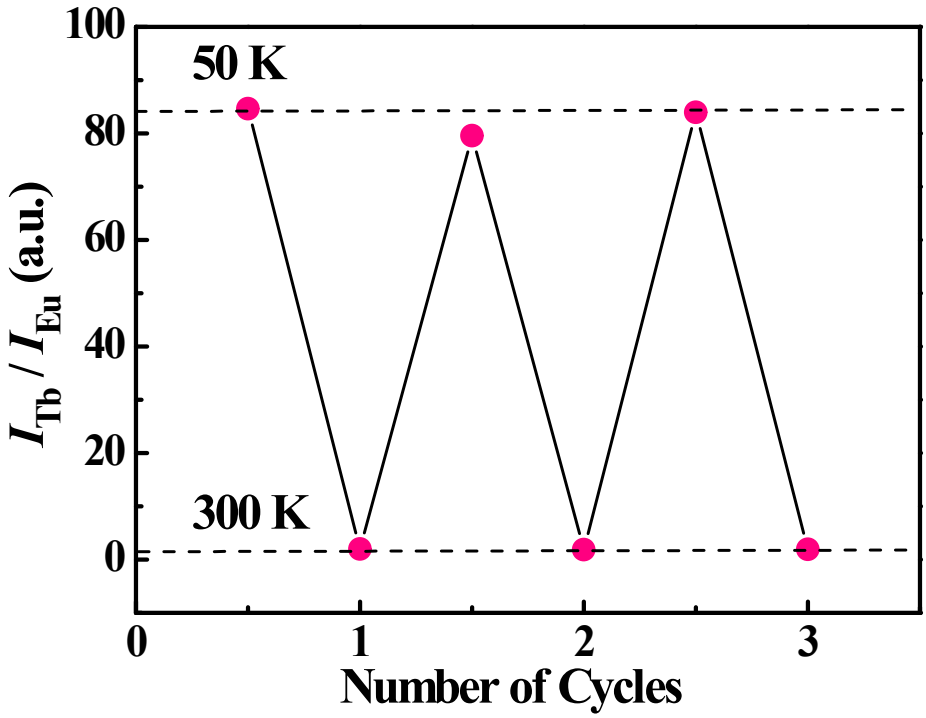

Figure S21. The reversible emission intensity ratio of Tb (544 nm) to Eu (614 nm) of $Eu_{0.001}Tb_{0.999}$(BPDC-2N) in cycles of heating and cooling.

References

1 C. Viravaux, O. Oms, A. Dolbecq, E. Nassar, L. Busson, C. Mellot-Draznieks, R. Dessapt, H. Serier-Brault and P. Mialane, *Journal of Materials Chemistry C*, 2021, **9**, 8323.

2 A. Cadiau, C. D. S. Brites, P. M. F. J. Costa, R. A. S. Ferreira, J. Rocha and L. D. Carlos, *ACS Nano*, 2013, **7**, 7213.

3 T. Xia, Y. Cui, Y. Yang and G. Qian, *Journal of Materials Chemistry C*, 2017, **5**, 5044.

4 Y. Cui, R. Song, J. Yu, M. Liu, Z. Wang, C. Wu, Y. Yang, Z. Wang, B. Chen and G. Qian, *Advanced Materials*, 2015, **27**, 1420.

5 V. Trannoy, A. N. Carneiro Neto, C. D. S. Brites, L. D. Carlos and H. Serier-Brault, *Advanced Optical Materials*, 2021, **9**, 2001938.

6 Y. Ding, Y. Lu, K. Yu, S. Wang, D. Zhao and B. Chen, *Advanced Optical Materials*, 2021, **9**, 2100945.

7 T. Feng, Y. Ye, X. Liu, H. Cui, Z. Li, Y. Zhang, B. Liang, H. Li and B. Chen, *Angewandte Chemie International Edition*, 2020, **59**, 21752.